

Internal Wave Attenuation by Coastal Kelp Stands

GEORGE A. JACKSON

Institute of Marine Resources, A-018, University of California, San Diego, San Diego, CA 92093

(Manuscript received 16 December 1983, in final form 2 April 1984)

ABSTRACT

Coastal kelp stands are a unique physical environment having high drag distributed throughout the water column. Temperature records from locations at increasing distances into the kelp show a damping of high-frequency variance and a slowing of wave propagation at low frequencies. This behavior at low frequencies is more a diffusion than a wave process. Linearized internal wave models incorporating linear drag successfully explain the frequency response of phase velocity but are less successful with the attenuation coefficient. The attenuation coefficient is well explained by the model of the outer area of the kelp but is overestimated in the kelp stand interior. In the outer area phase velocity is about 0.12 m s^{-1} at 100 cpd (cycles per day), a third of that at 1 cpd; attenuation coefficient is 7.5 km^{-1} at 100 cpd, 1.5 km^{-1} at 1 cpd.

1. Introduction

Internal wave attenuation has been studied for low-drag processes such as viscous shear and bottom friction (e.g. LeBlond, 1966; Crampin and Dore, 1970). There are regions along the California coast with high drag distributed relatively uniformly through the water column. These are the stands of the large seaweed, giant kelp. Growing in water as deep as 20 m, these seaweeds can decrease current velocities (Jackson and Winant, 1983). Such high drag areas can also have large effects on internal waves propagating through them.

Internal waves in the Southern California coastal region can be large relative to bottom depth. Isotherm fluctuations as large as 4 m in 15 m water depth are common (e.g., Lee, 1961). Their spectra show large peaks in the diurnal and semidiurnal frequencies (e.g. Cairns, 1968; Lee, 1961). In this shallow environment they move towards the land, perpendicular to shore (Lee, 1961). Their passage has been related to changes in cross-shore currents (Winant and Olson, 1976).

In this paper temperature records are presented which show a large damping effect of the kelp, *Macrocystis pyrifera*, on temperature fluctuations. Models are then developed for internal wave propagation in a high drag medium. Results from these models are in reasonable agreement with observed phase velocity and spectral energy changes.

2. Field observations

The kelp bed off Pt. Loma, San Diego is one of the largest kelp stands in Southern California. It stretches about 7 km along the coast and about 1 km offshore (Fig. 1). It is situated over a gently sloping

rock shelf which reaches 22 m bottom depth 1600 m from shore, drops to 30 m in an additional 100 m, and then merges into a shallow, downward-sloping sand bottom. The kelp bed grows to the surface from depths between ~6 and 30 m.

Kelp plants grow attached to hard bottom by a root-like holdfast. Vine-like fronds grow upward buoyed by small air bladders (pneumatocysts). At the surface, fronds spread out to form a canopy which can totally cover the surface. Each frond consists of rope-like stipe, about 1 cm in diameter, to which are attached the float-containing blades. The fronds of an individual plant bunch together to form a compact column between the bottom and the surface that typically may contain 40 stipes and is between 10 to 20 cm in diameter. Plant densities at the Pt. Loma bed ranged from 0.01 to 0.1 plants m^{-2} , with lower densities in deeper water. The drag for horizontal flow in this kelp stand is a factor of 10 greater than that of a non-kelp area and the currents about a tenth as energetic (Jackson and Winant, 1983). Kelp plant drag differs from bottom friction by being relatively uniform through the water column.

Temperature and current measurements were made using vector measuring current meters (VMCMs) on taut line moorings. The meters recorded average north- and eastward currents and temperature every 4 minutes. Further discussion of the instruments is given by Winant and Bratkovich (1981). Four VMCMs were located on a straight line perpendicular to shore over a total distance of 600 m, with instruments separated by intervals of about 200 m (Fig. 1). Temperature records extend from 24 September to 21 October, 1982. Root-mean-square current speeds ranged from 10.8 cm s^{-1} outside the bed at Station O to 5.8 cm s^{-1} just inside the bed at Station M, to

POINT LOMA KELP FOREST

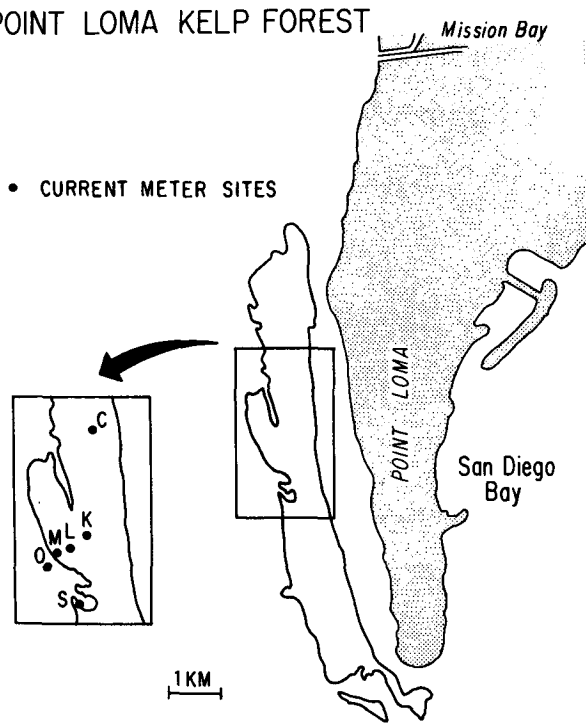


FIG. 1. Map of Pt. Loma kelp bed and station locations. Meter locations relative to outer edge of kelp bed, meter depth and bottom depth were: Station O—70 m outside, 6 m in 28 m bottom; Station M—120 m inside the kelp, 8 m in 17 m bottom; Station L—310 m inside, 6 m in 14 m bottom; Station K—530 m inside, 6 m in 14 m bottom.

2.2 cm s^{-1} in the middle of the bed at Station K (Jackson, 1983).

Buoyancy frequency was calculated from temperature profiles measured by divers using hand-held thermometers during the initial meter deployment. For a constant salinity of 33.5 ppt, maximum N is $2.8 \times 10^{-2} \text{ s}^{-1}$.

3. The temperature field

The temperature records show significant changes over distances of a few hundred meters (Fig. 2). There is a progressive smoothing of temperature fluctuations with increasing distance into the kelp that is indicative of diminishing high-frequency components in the kelp. Power spectra show this. There is little difference between spectra outside the bed at O and just inside at M (Fig. 3). High-frequency components are highly damped farther into the kelp, with variance dropping almost a factor of 10 at 100 cpd (cycles per day) in the 190 m between M and L. Coherence is high out to 100 cpd and phase varies systematically for temperature frequency components at adjacent locations.

There are two effects of kelp drag on the temperature fluctuations and therefore, on the internal waves. The first is an increasing damping with increasing frequency with relatively little damping at frequencies of 3 cpd or less (Fig. 4). The damping of high-frequency fluctuations is less between L and K, but

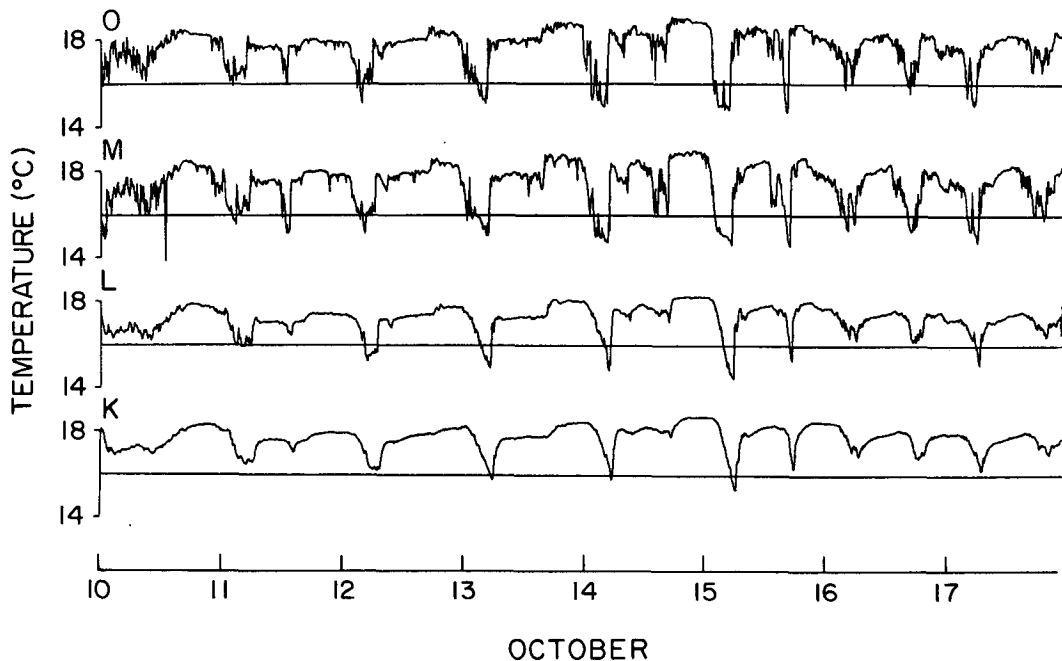


FIG. 2. Temperature records over part of the deployment. Data plotted are 8-minute averages. Data are presented in order of increasing distance into kelp.

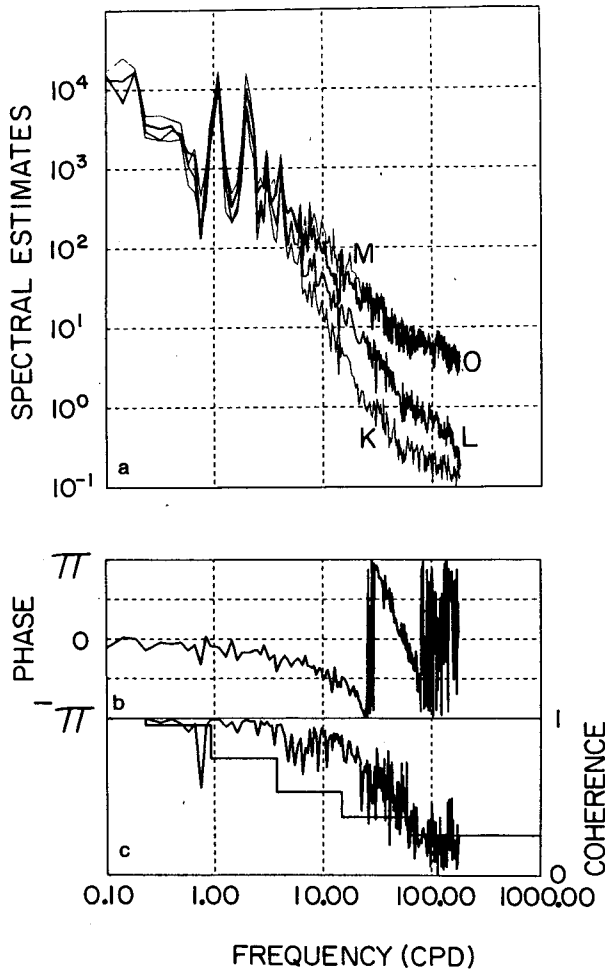


FIG. 3. Results of spectral analysis of temperature records: (a) variance spectra for the four locations. Data from locations O and M are indistinguishable, L and K substantially reduced. (b) Phase, and (c) coherence between L and K records. Stepped line represents 95% significance levels. Spectral components were band averaged.

high-frequency fluctuations are so reduced that this might result from lack of resolution of high-frequency variability in the highly damped record at K.

Concurrent with the damping of high-frequency variations there is a decrease in the horizontal phase speed c_H at low frequencies. Phase speed at the semidiurnal 2 cpd between O and M is too fast to calculate accurately with this sampling scheme but it is more than 20 cm s^{-1} . Within the kelp the phase speed at 2 cpd drops to about 5 cm s^{-1} , less than the 13 cm s^{-1} at 100 cpd (Fig. 4). Thus, the effect of damping by kelp over these 200 m intervals is to damp high-frequency fluctuations and slow low-frequency ones. (Note that phase speed calculations by this technique become unreliable when the wavelength is not greater than the station distance (Huang, 1981). Wavelengths are equal to or smaller than station spacing for frequencies greater than about 50 cpd.)

4. Internal wave propagation in presence of damping

The equations usually used to describe internal wave motions must be modified to describe propagation in a high-drag medium. The following sections show effects of drag on internal wave propagation in the case of two density layers and in the case of a constant density gradient. The equations include a linearized drag for horizontal momentum. Models shown have a two-dimensional, x - z geometry, which holds for waves traveling perpendicular to shore. There is the implicit assumption that the temperature-density structure is the same at all locations.

The models developed are adaptations of frictionless internal wave propagations in which bottom drag and viscous effects between water layers are neglected. The only drag addressed here is from the kelp. The justification for this, aside from analytic tractability, is that in a dense kelp stand bottom drag is small compared to kelp drag (Jackson and Winant, 1983).

a. Internal waves in a two-layer fluid

Consider a two-layered system, the upper layer with density ρ_1 and the lower layer with ρ_2 , the upper layer having a free surface with equilibrium at $z = 0$, the equilibrium boundary between the two layers of thicknesses H_1 and H_2 , and the bottom solid boundary at $-H$. For free surface displacement η and upward interface displacement h the momentum equations are (e.g., Gill, 1982)

$$u_{1t} = -g\eta_x - Du_1, \quad (1a)$$

$$u_{2t} = -\frac{\rho_1}{\rho_2}g\eta_x - g'h_x - Du_2, \quad (1b)$$

where D is the linearized drag coefficient, u_1 and u_2 are x -velocities in the upper and lower layers, and g' is the reduced gravity, $g' = g(\rho_2 - \rho_1)/\rho_2$. Continuity gives

$$(\eta + H_1 - h)_t + H_1 u_{1x} = 0, \quad (2a)$$

$$h_t + H_2 u_{2x} = 0. \quad (2b)$$

After eliminating u_1 , u_2 , the equations become

$$h_{tt} + h_t D - H_2(g - g')\eta_{xx} - g'H_2 h_{xx} = 0, \quad (3a)$$

$$(\eta_{tt} - h_{tt}) + D(\eta_t - h_t) - gH_1\eta_{xx} = 0. \quad (3b)$$

For solutions with $h = \mu\eta$ where μ is a constant these reduce to

$$\eta_{tt} + D\eta_t = c_e^2\eta_{xx}, \quad (4)$$

where $c_e^2 = gH_1/(1 - \mu) = \mu^{-1}[g - g'(1 - \mu)]H_2$.

For damped wave solutions of the form

$$\eta = A \exp[i(kx - \omega t) - \beta x], \quad (5)$$

where k , ω , and β are real,

$$k = (\omega/c_e)\gamma, \quad (6)$$

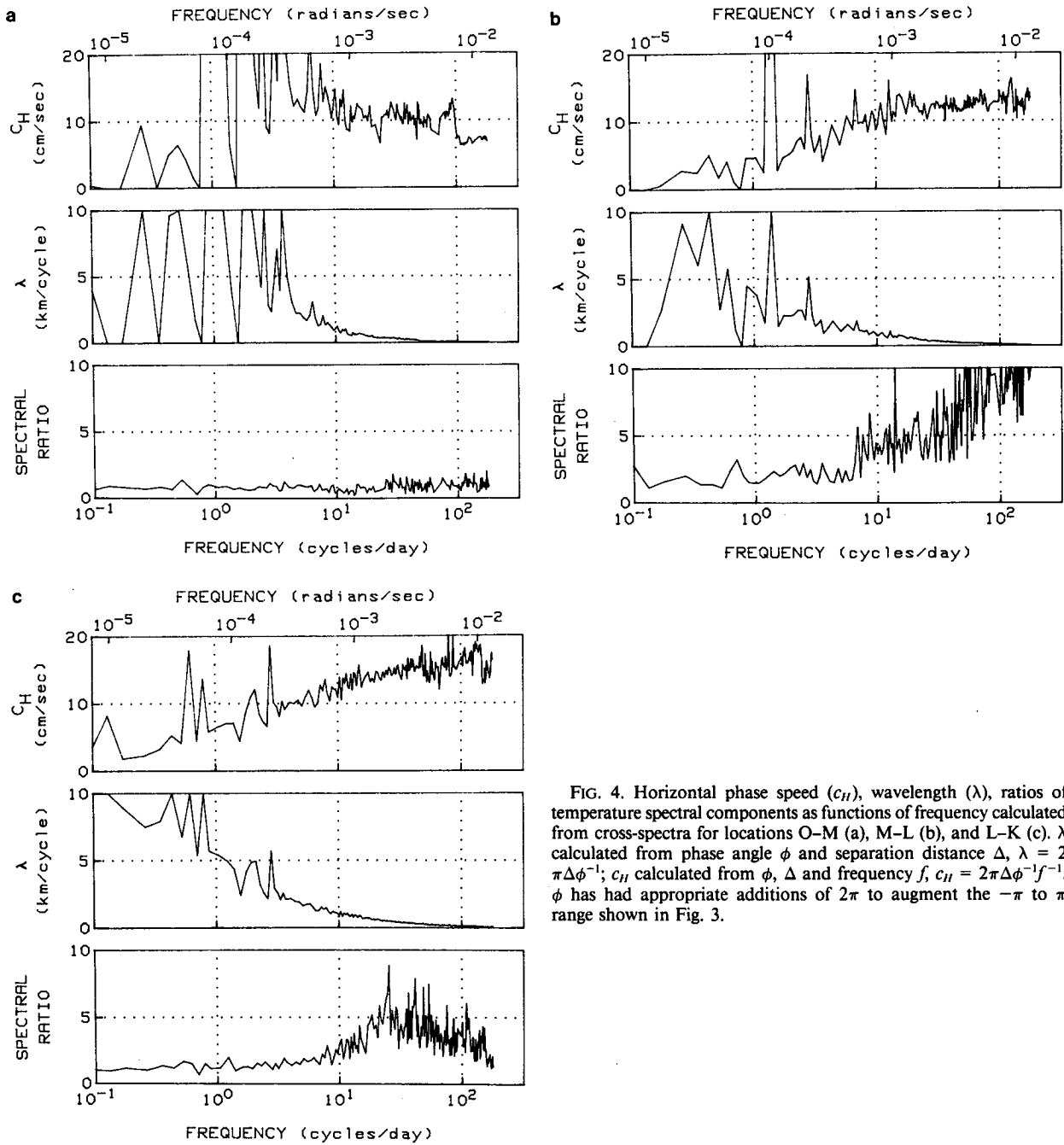


FIG. 4. Horizontal phase speed (c_H), wavelength (λ), ratios of temperature spectral components as functions of frequency calculated from cross-spectra for locations O-M (a), M-L (b), and L-K (c). λ calculated from phase angle ϕ and separation distance Δ , $\lambda = 2\pi\Delta\phi^{-1}$; c_H calculated from ϕ , Δ and frequency f , $c_H = 2\pi\Delta\phi^{-1}f^{-1}$. ϕ has had appropriate additions of 2π to augment the $-\pi$ to π range shown in Fig. 3.

where

$$\gamma \equiv \left[\frac{1}{2} + \frac{1}{2} (1 + D^2/\omega^2)^{1/2} \right]^{1/2}, \tag{7}$$

$$\beta = D(2c_e\gamma)^{-1}. \tag{8}$$

The horizontal phase speed c_H is then

$$c_H \equiv \omega/k = c_e\gamma^{-1}. \tag{9}$$

A dimensionless damping coefficient β/k is given by

$$\frac{\beta}{k} = \left(\frac{D}{2\omega} \right) \gamma^{-2}. \tag{10}$$

The term γ incorporates the frequency-dependent effect of drag and is the only drag-affected term for c_H and k . For zero drag, $\gamma = 1$, $c_H = c_e$ and $\beta = 0$. This is the expected zero-drag case. For low frequencies, $D \gg \omega$,

$$\gamma \approx \left(\frac{D}{2\omega}\right)^{1/2}, \quad (11a)$$

$$\beta \approx (\omega D/2)^{1/2}/c_e, \quad (11b)$$

$$c_H \approx c_e(2\omega/D)^{1/2}, \quad (11c)$$

$$\beta/k \approx 1. \quad (11d)$$

For high frequencies, $D \ll \omega$,

$$\gamma \approx 1 + \frac{1}{8} D^2/\omega^2, \quad (12a)$$

$$\beta \approx \frac{D}{2c_e}, \quad (12b)$$

$$c_H \approx c_e, \quad (12c)$$

$$\beta/k \approx \frac{D}{2\omega}. \quad (12d)$$

These show that β and c_H are less for low frequencies.

There are two possible values for c_e in the two-layer model (Gill, 1982). The larger value is for the case where surface and density interface displacements are in phase, corresponding to the barotropic mode; the smaller value is the baroclinic mode. In the limit of no density difference between top and bottom layer the barotropic mode becomes a surface wave with $c_e = (gH)^{1/2}$. For the baroclinic mode, $c_e \approx (g'H_1H_2/H)^{1/2}$.

b. Internal waves in a constant density gradient

For the case of a constant vertical density gradient in an incompressible Boussinesq fluid, the appropriate equations are (e.g. Gill, 1982)

$$u_t = -\rho_0^{-1}p'_x - Du, \quad (13a)$$

$$w_t = -\rho_0^{-1}p'_z - (\rho'/\rho)g, \quad (13b)$$

$$\rho'_t + w\rho_{0z} = 0, \quad (13c)$$

$$u_x + w_z = 0, \quad (13d)$$

where u and w are horizontal and vertical velocities, p' is the perturbation pressure, ρ' is the perturbation density, and $N^2 = -g\rho_0^{-1}\rho_{0z}$ is the square of the buoyancy frequency. With the approximation $\rho_0^{-1}(\rho_0 w_z)_z \approx w_{zz}$, these reduce to

$$Dw_{izz} + (w_{xx} + w_{zz})_t + N^2 w_{xx} = 0. \quad (14)$$

For a damped wave solution of the form

$$w = A \exp[i(kx + mz - \omega t) - \beta x], \quad (15)$$

where k , m , ω , and β are real coefficients, the following hold

$$\omega^2 = \frac{N^2(k^2 - \beta^2)}{k^2 + m^2 - \beta^2}, \quad (16a)$$

$$\beta = \frac{1}{2} D(\omega/k)m^2(N^2 - \omega^2)^{-1}. \quad (16b)$$

For the case where $\omega^2/N^2 \ll 1$ and $m^2 \gg (k^2 - \beta^2)$, these reduce to

$$k = (m/N)\omega\gamma, \quad (17a)$$

$$\beta = \frac{1}{2} D(m/N)\gamma^{-1}, \quad (17b)$$

$$\beta/k = \frac{1}{2} (D/\omega)\gamma^{-2}, \quad (17c)$$

$$c_H \equiv \omega/k = (N/m)\gamma^{-1}, \quad (17d)$$

where γ was defined in Eq. 7. These are the same results as in the 2-layer model (Eqs. 6–10) but with the no-drag phase velocity c_e equal to (N/m) . High- and low-frequency limits are the same as in Eqs. 11–12.

For the case of a water column of depth H , m is constrained to $\pi n/H$ where n is an integer, here non-zero because of the assumption of $\omega^2 \ll N^2$.

5. Discussion

The results of these two models show that both c_H and β decrease with decreasing ω . This agrees with the qualitative discussion in Section 3 that the temperature variance at 100 cpd is more heavily damped than that at 2 cpd but the phase speed is more affected at 2 cpd. The value of β decreases with increasing c_e but fractional change in phase speed is the same regardless of c_e . This implies that barotropic waves will, because of their high undamped phase velocities, pass through a kelp stand undamped but slowed. Surface gravity waves with their high frequencies, $\omega \sim 0.1 \text{ s}^{-1}$, should not even be slowed. Interestingly, a dimensionless attenuation, β/k , is independent of c_e and actually increases with decreasing ω .

The differential equation describing amplitude propagation (Eq. 4) is a combination diffusion-wave equation. For high frequencies ($\omega \gg D$) η_{tt} is larger than $D\eta_t$ and the equation is more of a wave equation; for low frequencies ($D \ll \omega$) it is more of a diffusion equation. Thus, for low frequencies, the propagation of an oscillating signal is more a diffusion process into the attenuated medium than an actual wave propagation. Le Blond (1978) has described a similar situation where tidal propagation in shallow waters is more diffusion than wave propagation.

For an internal wave propagating in a constant gradient, c_e is a function of N and the vertical wave number m . Smaller N and larger m lead to lower c_e and therefore increased β . The first internal mode ($n = 1$) in the finite depth case has the smallest value and is therefore the least damped mode. Higher modes should be more rapidly attenuated.

To compare the calculated damping and phase speed there need to be values for c_e and D . These can be compared to values calculated from T spectra at the different stations. The spectral data have already been used to calculate phase speeds (Fig. 4). Atten-

uation coefficients can be calculated if the T -fluctuation at any ω is proportional to η - and w -fluctuations. Then, because T variance is proportional to the square of the Fourier coefficient,

$$\beta_{\text{obs}} = (\Delta x)^{-1} \ln(S_1/S_2), \quad (18)$$

where S_1 and S_2 are the power spectral components for frequency ω at Station 1 and 2 which are separated by Δx . Values of β_{obs} are as high as 0.005 m^{-1} at 100 cpd between M and L (Fig. 5).

Values of c_e and D can be estimated independently of the temperature records. For the constant density-gradient model, c_e can be calculated using the density gradient and station depth. The few temperature profiles taken during the installation of the current meters show constant density gradients over much, but not all, of the water column (Fig. 5). For a uniform density gradient given by 19° at the surface and 16° at 15 m, N is $2.16 \times 10^{-2} \text{ s}^{-1}$. The resulting value of c_e is 0.11 m s^{-1} for the first internal mode in water 16.5 m deep. A linearized drag coefficient for D can be calculated as the product of the square-law drag coefficient for the Pt. Loma kelp measured during February 1981, 0.01 m^{-1} (Jackson and Winant, 1983), and average rms current speed between two stations. Between M and K the rms current speed was about 0.043 m s^{-1} ; between L and K it was about 0.022 m s^{-1} . The values of D are then 4.3×10^{-4} between M and L and $2.1 \times 10^{-4} \text{ s}^{-1}$ between L and K.

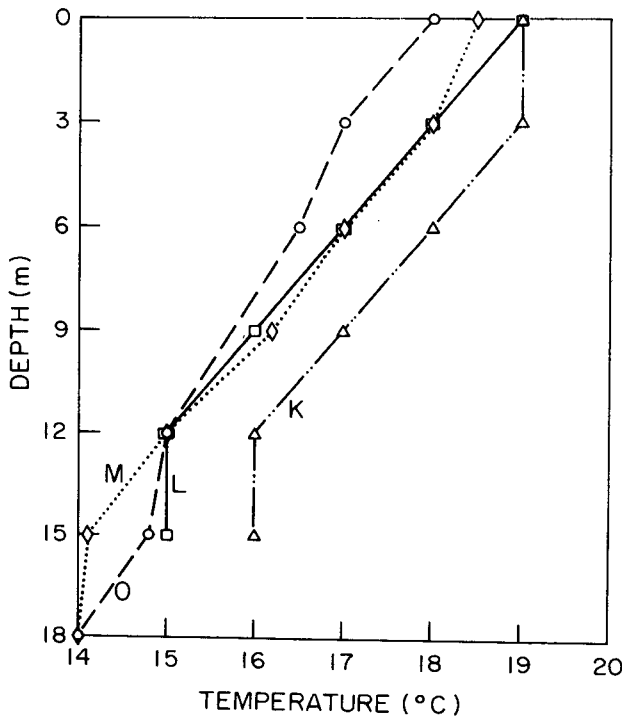


FIG. 5. Temperature profiles at the station locations at the time of deployment, 24 September 1982. Letters indicate the stations.

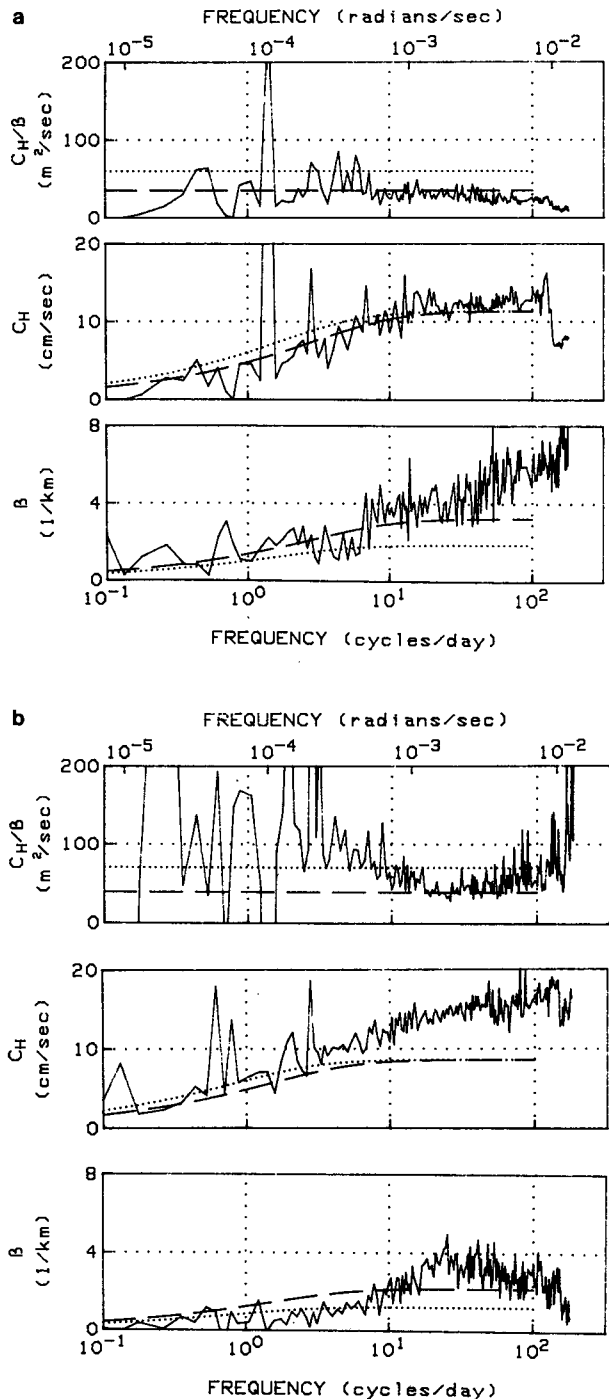


FIG. 6. Attenuation coefficient (β) and phase speed, (c_H) and their ratio (c_H/β), as functions of frequency. All calculations are for the first internal mode. (a) Between Stations M and L $m = 0.19 \text{ m}^{-1}$, $N = 2.16 \times 10^{-2} \text{ s}^{-1}$, $c_e = 0.11 \text{ m s}^{-1}$. Solid line: from T spectra; Dotted line: $D = 4.3 \times 10^{-4} \text{ s}^{-1}$ (original D calculated); Dashed line: $D = 7.4 \times 10^{-4} \text{ s}^{-1}$ (D modified to account for interannual changes). (b) Between Stations L and K $m = 0.25 \text{ m}^{-1}$. Solid line: from T -spectra; Dotted line: $D = 2.1 \times 10^{-4} \text{ s}^{-1}$, $N = 2.16 \times 10^{-2} \text{ s}^{-1}$ (original D , N calculated); Dashed line: $D = 3.74 \times 10^{-4} \text{ s}^{-1}$, $N = 2.16 \times 10^{-2} \text{ s}^{-1}$ (modified to account for interannual changes). The theories predict that c_H/β should be independent of frequency.

Comparison of predicted and observed values of c_H and β between M and L shows that c_H is well predicted throughout the frequency range but that the predicted β is too low (Fig. 6a). This prediction could be low if natural variations in kelp density altered the kelp stand drag between the time the original drag calculation was made (February 1981) and the time that the measurements described in this paper were made (September–October 1982). There is evidence that this happened. To the extent that currents at O and K respond to the same pressure fields, the ratio of rms currents at O and K is a measure of the relative size of the square-law drag coefficient in the kelp. This ratio was 12.63 for the 1981 deployment and 22.46 for the 1982 deployment. This implies that the linearized drag coefficient D for this study should be 0.78 larger than the one found earlier. That is, $D = 7.7 \times 10^{-4} \text{ s}^{-1}$. Recalculation of c_H and β using this value of D yields a good fit to the data (Fig. 6a). Further minor improvements can be made by tinkering with the value of N or using a slightly higher rms current speed for the linearization. Regardless of this fine-tuning, the theory predicts that the ratio c_H/β should be constant over the frequency range regardless of the actual values of c_e or D and it is. The model works well in this region.

The situation is more complicated between L and K. The value of c_e should decrease from that between M and L because the shallower bottom depth increases the value of m . Instead, a value of c_e higher than between M and L is needed to fit the c_H curve (Fig. 6b). Such an increase in c_e could occur if the density gradient were sharper in shallower water. The model still predicts the general changes in phase velocity over the frequency range calculated. The attenuation coefficient is poorly predicted (Fig. 6b). This is not because of poor estimates of D or N or because of a loss of resolution of the T signal at high frequencies. Rather, there is a fundamental problem. The theories predict that the ratio c_H/β should be constant. However, the observations show a systematic increase of the ratio with decreasing frequency for the region between L and K. The linear theories work poorly in this region.

Thus, the simple linear theories developed here work well at explaining changes in internal waves propagating through a high-drag coastal area in the outer area, not as well farther in. These theories do predict the frequency-dependence of horizontal phase velocity throughout but overestimate the attenuation coefficient in the interior, especially in its frequency dependence. That the simple linear theories do not completely describe internal wave attenuation in the complex coastal area is not surprising; that they do

describe phase velocities throughout the attenuation in a more active area is.

6. Conclusion

The high-drag areas of a coastal kelp bed slow and dampen internal waves propagating through. Horizontal phase velocities are slower for low-frequency waves than for high. At 1 cpd they are about a third of what they are at 100 cpd. Attenuation coefficients range from about 0.005 m^{-1} at 100 cpd to about 0.0015 m^{-1} at 1 cpd. Simple linear theories adequately explain the variation in phase velocity but can overestimate attenuation coefficients at low frequencies.

Acknowledgments. The author acknowledges the help of C. Winant, D. Wahlberg, P. D'Acri and M. Kirk in acquiring the data and E. Stewart in analyzing them. R. Davis, R. Pinkel and C. Cox provided useful discussions, reviewers provided helpful comments. M. Ogle helped with manuscript preparation. This work is a result of research sponsored in part by NOAA, National Sea Grant College Program, Department of Commerce, under Grant NA80AA-D-00120, through the California Sea Grant College Program, and in part by the California State Resources Agency, Project R/CZ-59. The U.S. Government is authorized to produce and distribute reprints for governmental purposes.

REFERENCES

- Cairns, J. L., 1968: Thermocline strength fluctuations in coastal waters. *J. Geophys. Res.*, **73**, 2591–2595.
- Crampin, D. J., and B. D. Dore, 1970: Numerical comparisons of the damping of internal gravity waves in stratified fluids. *Pure Appl. Geophys.*, **79**, 53–65.
- Gill, A. E., 1982: *Atmosphere-Ocean Dynamics*. Academic Press, 662 pp.
- Huang, N. E., 1981: Comments on 'Modulation characteristics of sea surface waves' by A. Ramanonjiarisoa and E. Mollo-Christensen. *J. Geophys. Res.*, **86**, 2073–2075.
- Jackson, G. A., 1983: The physical and chemical environment of a kelp community. *Effects of Waste Disposal in Kelp Communities*, W. Bascom, Ed. South. Calif. Coastal Water Res. Proj., Long Beach, 11–37.
- , and C. D. Winant, 1983: Effect of a kelp forest on coastal currents. *Cont. Shelf Res.*, **20**, 75–80.
- LeBlond, P. H., 1966: On the damping of internal gravity waves in a continuously stratified ocean. *J. Fluid Mech.*, **25**, 121–142.
- , 1978: On tidal propagation in shallow rivers. *J. Geophys. Res.*, **83**, 4717–4721.
- Lee, O. S., 1961: Observations on internal waves in shallow water. *Limnol. Oceanogr.*, **6**, 312–321.
- Winant, C. D., and J. R. Olson, 1976: The vertical structure of coastal currents. *Deep-Sea Res.*, **23**, 925–936.
- , and A. W. Bratkovich, 1981: Temperature and currents on the Southern California Shelf: A description of the variability. *J. Phys. Oceanogr.*, **11**, 71–86.